Int J Legal Med (1998) 111 : 314–319

ORIGINAL ARTICLE

B. Karger · Z. Puskas · B. Ruwald · K. Teige
G. Schuirer

Morphological findings in the brain after experimental gunshots using radiology, pathology and histology

Received: 22 December 1997

Abstract The tissue disruption inside the brain after experimental gunshots to the head was investigated with special reference to secondary bone missiles and intracranial pressure effects such as cortical contusion and deep intracerebral haemorrhages. The evidential value of various examination methods is compared. 9 mm Parabellum ammunition was fired to the temporal region of calves (n = 10) from a distance of 0–10 cm. Plain film radiography, CT, MRI, visual inspection and histology were performed on every brain. The tissue disruption of the permanent tract is delineated best by artefact-free MRI. Cortical contusions and deep intracerebral haemorrhages were detected infrequently by visual inspection and imaging techniques although they were present in every brain as verified by histology. These injuries remote from the tract increase cerebral wounding compared to non-confined tissue. In particular, the brain stem and central areas were frequent sites of haemorrhages, which can be expected to have serious and immediate consequences. Ectopic bone fragments were found in all brains using CT scans. Bone fragments were located inside clearly enlarged permanent tracts or were driven into brain tissue. In the latter cases, secondary shot channels up to 4 cm in length could be verified by histology. Cortical contusions and intracerebral haemorrhages can only be detected reliably by histology. The localization of bone fragments requires CT scans. Therefore, a detailed examination is accomplished best by a combination of the methods applied in this study.

B. Karger (✉) · K. Teige
Institute of Legal Medicine, University of Münster,
Von-Esmarch-Strasse 62, D-48129 Münster, Germany
Fax: +49 251 8355158

Z. Puskas · G. Schuirer
Institute for Clinical Radiology, University of Münster,
Albert-Schweitzer-Strasse 48, D-48129 Münster, Germany

B. Ruwald
Royal Danish Armed Forces, Veterinary Corps, Denmark

Key words Wound ballistics · Gunshots to the head · Brain · Histology · Radiology

Introduction

Penetrating gunshots to the head carry a high early mortality rate of 90% or more (Kaufman et al. 1986; Siccardi et al. 1991). In addition to the vital significance of the central nervous system, the head offers special wound ballistic features. The penetration of the skull can generate secondary bone missiles (Kirkpatrick and DiMaio 1978; Finnie 1993) and the confined intracranial space provided by the non-yielding skull hampers the free expansion of the temporary cavity (Karger 1995). Consequently, intracranial overpressure is elevated compared to isolated tissue (Watkins et al. 1988; Dittmann 1989). The expanding temporary cavity and the counterpressure from the skull enhance compression and shearing of cerebral tissue (Karger 1995). This can lead to cortical contusion (Spatz 1941; Freytag 1963; Henn and Liebhardt 1969; Kirkpatrick and DiMaio 1978) and intracerebral haemorrhages remote from the trajectory (Allen et al. 1982; Finnie 1993; Besenski et al. 1995). In addition, intracranial overpressure can result in indirect skull fractures predominantly located in the anterior cranial fossa (Klaue 1949; Karger 1995). This comparative study investigates the morphology and incidence of these intracerebral injuries independent of direct crushing of tissue by the bullet in an experimental model using radiological, macroscopical and histological methods.

Material and methods

The detailed experimental set-up is described in a previous publication (Karger et al. 1996). Live New Jersey calves (n = 10), 5–6 months old and all destined for slaughter, were shot into the right temple by a veterinarian licensed to perform livestock slaughter. The pistol was a 9 mm SIG P210 and two types of ammunition were used: a conventional 9 × 19 mm Luger full metal jacket (FMJ) round nose (RN) bullet (mass 7.5 g) produced by AMA (n = 6) and a 9 × 19 mm Luger Action-1 bullet (hollow point, solid copper-alloy bullet, 5.4 g) produced by Dynamit Nobel AG (n = 4). The range of fire was 0–10 cm and the transverse trajectories were directed towards the left temporal region. The muzzle velocity of both types of projectiles was measured by Doppler Radar (Knudsen and Svender 1994) by averaging the results of 10 additional shots using the same pistol and one lot of ammunition. In two cases, the exit velocities of FMJ bullets were also recorded.

The gunshots were followed by complete autopsies of the heads including soft tissue dissection and examination of the skull. After removal, the brains were fixed in buffered 4% formaldehyde. The isolated fixed brains were then examined by radiology: plain film radiographs were taken in the axial view using a conventional mammography device, 10 mm coronal CT scans with high resolution (512 × 512 pixel, 120 mm field of view) and maximum radiation exposure (110 KV, 500 mAS) were performed on a Siemens Somatom AR and axial, coronal and sagittal MR scans were performed on a Siemens Magnetom SP at 1.5 Tesla (PDw, T2 and T1w axial conventional spin echo, sagittal T1w MPRAGE, axial T2*w FLASH 2D, coronal and axial T2w TSE). Subsequently, the brains were cut into 1 cm thick coronal slices parallel to the trajectory. The slices were photographed and measured. Tissue for histology was collected according to a standard scheme from the temporal, frontal and occipital lobes, the cerebellum, the midbrain, the diencephalon, the pons, the medulla oblongata, the upper cervical spinal cord, the entrance and exit regions and from the vicinity of the permanent tract. Tissue showing indication of injury was collected in addition. The samples were embedded in paraffin wax, sectioned at 6 μm, and stained with HE, Azan and Masson for examination with light microscopy. If bone fragments were suspected, decalcification was performed in advance.

Results

The mean muzzle velocities were 372 m/s (FMJ) and 432 m/s (Action-1). The bullets perforated the thick temporal muscle (3–4 cm) before penetrating the cranium. The expanded deformation zone of the Action-1 bullets fragmented during impact with the bone and remained outside the cranium. The temporal bone was 5–7 mm thick and the sutures were closed but represented points of mechanical weakness. Indirect skull fractures, which were present in every case, were restricted to the sutures. The brain volume varied between approximately 400 and 500 cm^3 and the heads were 17–21 cm wide. All Action-1 bullets lodged in the bone or below the skin at the exit side, whereas all FMJ bullets perforated the head and left with an exit velocity of approximately 120 m/s (2 recordings). All calves collapsed immediately.

Plain film radiographs provided an overview of intracerebral bone fragments (Fig. 1). The size and the location of the bone fragments could be determined exactly by CT examination (Fig. 2). Two groups of bone fragments

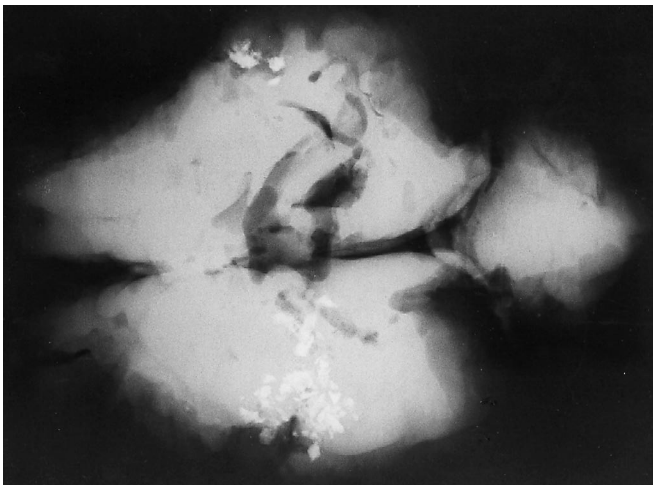

Fig. 1 Plain film radiography of a calf brain, axial view. FMJ bullet, contact shot. The number of bone fragments is higher at the entrance defect (below) than at the exit defect (above)

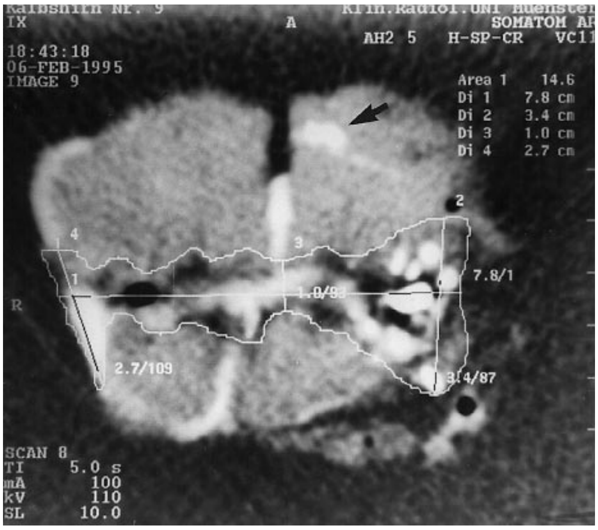

Fig. 2 Coronal CT scan. Action-1, range of fire 5 cm. The drawn lines do not delineate the zone of tissue disruption exactly because of adjacent edema and hematoma. Bone fragments accumulated at the entrance defect (right side). One fragment at a distance from the tract with adjacent haemorrhage is marked by the arrow. Blood is located inside the tract, the subarachnoidal space and at the exit defect

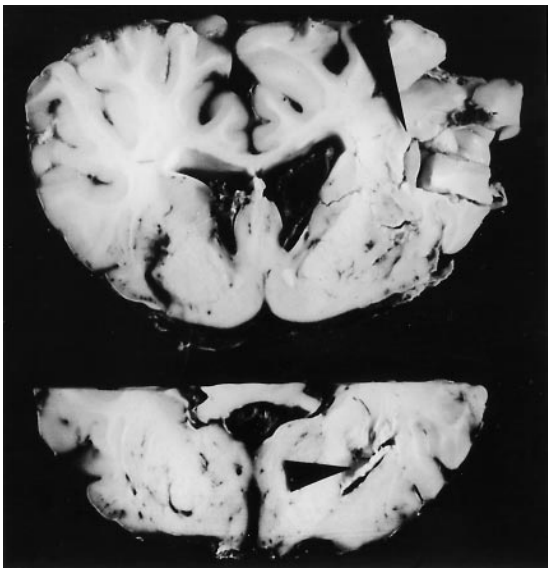

Fig. 3 Coronal brain slices showing two large intracerebral bone fragments marked by arrows at a distance of 2–3 cm from the tract. The ventricles are filled with blood and both thalami (lower slice) show petechial haemorrhages. FMJ bullet, range of fire 10 cm

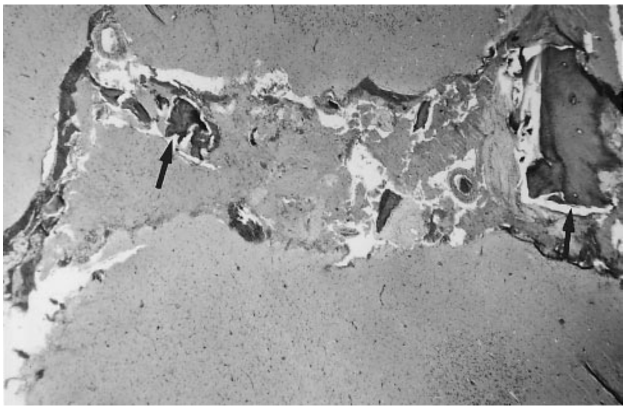

Fig. 4 A retracted secondary shot channel with haemorrhage and lacerated brain tissue. The underlying intracerebral bone fragments are marked by arrows. HE, × 38

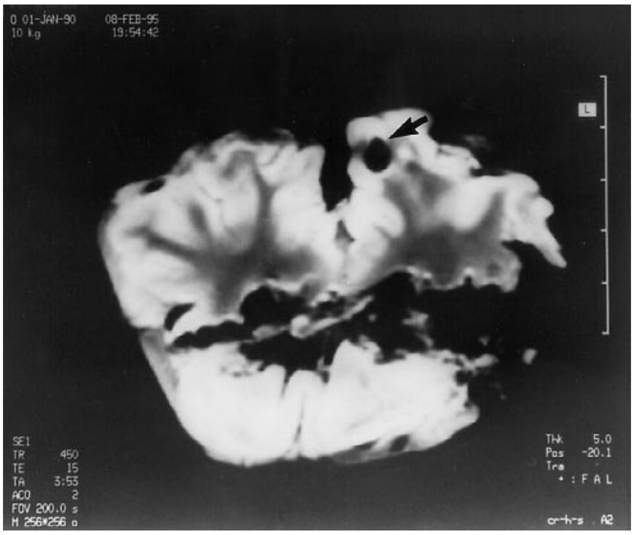

Fig. 5 Coronal MR scan of the same brain shown in Fig. 2. The zone of tissue disruption is clearly shown. The bone fragment marked by the arrow induced focal signal loss (compare Fig. 2). Action-1, range of fire 5 cm

Fig. 6 Intracerebral petechial haemorrhages in a symmetrical distribution in both thalami at a distance of approximately 3 cm from the tract. The third ventricle is filled with blood. FMJ bullet, contact shot

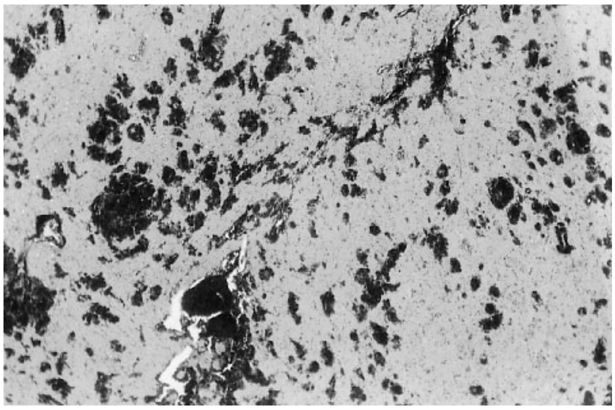

Fig. 7 A tight pattern of haemorrhages in the left thalamus comprising some ball haemorrhages and multiple patchy structures. The appearance with the naked eye is shown in Fig. 6. HE, × 38

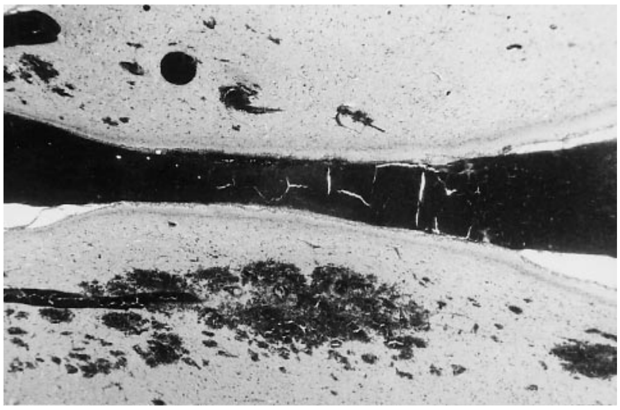

Fig. 8 Deep cerebral haemorrhages in the form of a fine ”cloudy” pattern (below) and ball haemorrhages (above) around the third ventricle which is filled with blood. HE, × 38

could be distinguished with regard to the location relative to the wound tract. In 6 out of the 10 cases, intraluminal bone fragments accumulated inside a bulge of the tract causing a clear enlargement of the tissue disruption. In addition bone fragments of varying size were always found inside brain tissue. The preferential location was close to the entrance defect (Figs. 1, 2) but bone fragments could also be verified in front of the exit defect (Fig. 1) and along the trajectory at a distance of up to 4 cm from the permanent tract (Figs. 2, 3). Histological examination showed bone chips surrounded by haemorrhages and lacerated or compressed neural tissue. If the brain was cut in the appropriate plane, bloody and retracted secondary shot channels including the underlying fragment and lacerated brain tissue could be demonstrated (Fig. 4). Small bone fragments visible on CT scans frequently eluded detection by visual inspection, palpation or histology. Secondary shot channels could only be verified by histology.

The type of ammunition used (FMJ vs Action-1) and the range of fire (contact vs close-range) did not have a clear effect on the resulting cerebral injury. The irregularly shaped permanent tracts were surrounded by lacerated brain tissue and by a small zone of extravasation. The

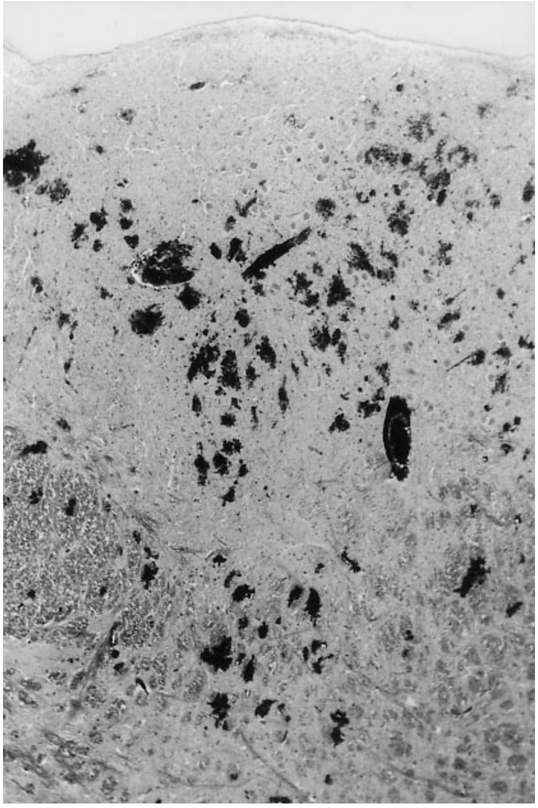

Fig. 9 A patchy pattern of haemorrhages in the brain stem close to the rhomboid fossa (above). Masson, × 62

Fig. 10 Irregularly shaped perivascular haemorrhages in the posterior horn of the upper cervival spinal cord. Masson, × 62

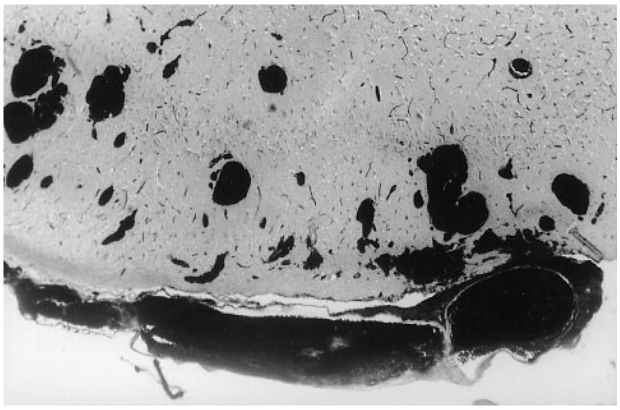

Fig. 11 Cortical contusion at the base of the frontal cortex in the form of ball haemorrhages. The extensive dilation of capillary vessels produces fine thread-like structures. Blood in the subarachnoidal space. HE, × 62

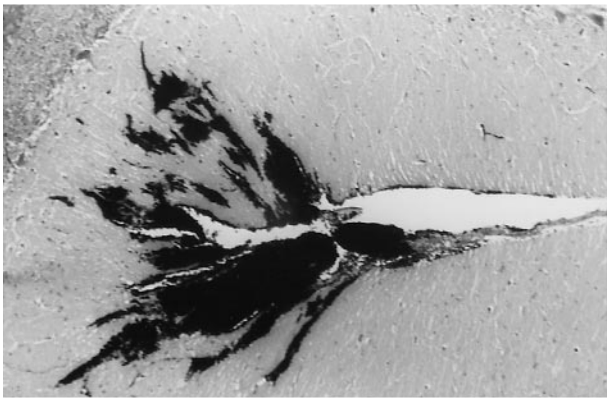

Fig. 12 Cortical contusion in the cerebellar cortex presenting as a directed striated pattern similar to a spider burst or a broom. The morphology suggests the dynamic force applied. HE, × 156

delineation of the permanent tract could be visualized clearly by MRI (Fig. 5) as long as no susceptibility artefacts due to ferromagnetic foreign bodies (minute metallic scatter from both types of bullets) or focal signal loss due to artificially formed air bubbles occurred. Bone fragments also induced artefacts which impeded the visualization of these fragments by MRI (Fig. 5). CT scans did not provide a clear distinction of necrotic and non-necrotic tissue due to adjacent edema and blood (Fig. 2).

Intracerebral haemorrhages remote from the tract could be verified in all brains by histology and sometimes by visual inspection (Figs. 3, 6) or CT. Apart from typical perivascular ring or ball haemorrhages, patchy and irregularly-shaped haemorrhages also occurred (Figs. 7–10). Preferential locations were central and caudal parts of the brain, especially the thalami (Fig. 7), the basal ganglia and the brain stem. Haemorrhages in the brain stem (Fig. 9) or the upper cervical spinal cord (Fig. 10) could be verified by histology in 7 out of the 10 cases.

Contusion of the cerebral cortex could only be demonstrated infrequently by radiology or visual inspection. However, cortical contusion zones were present in every brain as verified by histology (Fig. 11). Preferential locations were the basal cortex of the cerebrum (Fig. 11) and of the cerebellum (Fig. 12). In two cases, haemorrhages could be detected in the cerebellopontile angle. The morphology of the contusions varied from ball haemorrhages (Fig. 11) to a peculiar striated pattern (Fig. 12).

Discussion

Imaging techniques are used frequently in the investigation of fatal and non-fatal intracranial gunshot wounds

(Wülleneweber et al. 1977; Cooper et al. 1979; Schmidt and Kallieris 1982; Seidel et al. 1983; Schumacher et al. 1984; Rodieck 1984; Messmer and Fierro 1986; Metter et al. 1988; Hollerman et al. 1990; Teitelbaum et al. 1990; Smith et al. 1991; Harris 1991; Besenski et al. 1995). Bullets and ectopic bone can be detected by plain film radiographs in two planes but if the brain is not isolated, small foreign bodies and those located in the vicinity of the base of the skull can elude detection due to masking. Therefore, the total number and the localization of bone fragments could only be determined by CT scans. Contrary to previous investigations, intracerebral bone fragments could be verified in every case. In a large series of 154 haemodynamically stable patients, Besenski et al. (1995) were able to demonstrate bone fragments by CT scans in 67% but the majority of wounds were from small shell fragments. Other studies (Cooper et al. 1979; Rodiek 1984; Schumacher et al. 1984) reported intraparenchymal bone fragments in most cases. The fact that bone fragments were always detected in this series may be due to improved imaging techniques, the small number of cases or the use of an experimental model involving large-calibre handgun bullets and the examination of isolated brains. The final location of the bone fragments relative to the wound tract shows that bone can be driven into brain tissue (Fig. 3) but can also be found inside the wound tract, which indicates that these intraluminal fragments did not leave the temporary cavity. Both forms of secondary missiles resulted in additional injury to the brain. Intracerebral bone fragments caused secondary shot channels lacerating brain tissue (Fig. 4) and intraluminal fragments increased the diameter of the permanent tract.

The delineation of the tissue disruption of the permanent tract was the major advantage of artefact-free MRI (Fig. 5) over CT scans (Fig. 2). The determination of the direction of fire, i.e. the differentiation of entrance and exit wounds, can be assisted by the location of intracerebral bone fragments, which usually accumulate behind the entrance defect. It should be noted, however, that bone fragments can also travel in a direction against the line of fire (Lorenz 1948) so that intracerebral bone can also be located at the side of the exit defect (Fig. 1; Rodieck 1984; Schumacher et al. 1984). The expanding muzzle gases in the contact shots did not increase the tissue disruption inside the brain compared to close-range shots. Although this might be due to the wide subcutaneous space in the calves, Kirkpatrick and DiMaio (1978) reported the same finding in humans.

Morphological consequences of intracranial pressure effects have rarely been investigated. Intracerebral haemorrhages could be verified by a thorough histological examination in every brain. Allen et al. (1982) and Finnie (1993) also found perivascular ball haemorrhages remote from the tract by light microscopy but did not describe the patchy and irregularly-shaped haemorrhages (Figs. 7–10) present in this study. The preferential locations in the central and caudal parts of the brain correspond to previous investigations (Allen at al. 1982; Finnie 1993; Besenski et al. 1995). In particular, haemorrhages were frequently detected in the central grey zones and the brain stem but extended even down to the upper cervical spinal cord (Figs. 3, 7–10). Cooper et al. (1979) and Seidel et al. (1983) reasoned that shock waves (sonic pressure waves) impacting the brain stem were responsible for these haemorrhages. But the duration of the high shock wave amplitudes is too short to move or injure tissue (Harvey et al. 1947; Fackler and Peters 1991). Therefore, haemorrhages cannot be caused by shock waves produced by gunshots. Instead, intracranial temporary cavitation results in compression and shearing of the brain tissue and the foramen magnum represents a pre-existing vent in the skull. Consequently, the displacement and shearing of tissue is most pronounced in front of the vent where pressure gradients accumulate, i.e. in the central brain, and the brain stem can be driven into the foramen magnum and against the rims and edges. The resulting vascular (and neuronal) injury is likely to cause severe effects in this small but significant area. It probably represents the morphological correlative to the very rapid cardiovascular and respiratory “brain stem effects”, which have been reported in pathophysiological animal studies of craniocerebral gunshot wounds (Crockard et al. 1977; Levett et al. 1980; Carey et al. 1989) and to the immediate collapse witnessed in the calves. A secondary development of intracerebral haemorrhages due to clinically elevated pressure from edema or haematoma is possible (Illchmann-Christ 1951; Petersohn 1967) but can be excluded in this series because of the rapid central death with extremely short survival time.

Histological examination showed that cortical contusion zones as a result of the brain surface impacting against the skull were present in every brain. Freytag (1963), Henn and Liebhardt (1969) and Kirkpatrick and DiMaio (1978) reported preferential locations at the base of the cerebrum and cerebellum, which is corroborated by this study. The paucity of reports including microscopical investigations renders a comparison with the literature difficult. In addition to grouped ball haemorrhages (Fig. 11), the morphology of contusions also presented in the form of a longitudinal pattern in the cortical layer (Fig. 12) indicating the dynamic mechanism of development.

In conclusion, the combination of initial fixation of the brain, imaging techniques (especially CT), patho-anatomy and histology made it possible to demonstrate secondary missiles (bone fragments), cortical contusions and deep intracerebral haemorrhages in every brain investigated. These additional injuries increase cerebral wounding and also occur in areas of high functional significance. The brain volume of calves is smaller compared to humans and the resulting higher intracranial pressure peaks may have enhanced the cavitation-dependent injuries. However, the same findings have been demonstrated in humans. In case work, the various methods applied in this study can be used if a case offers special features or if additional medico-legal questions such as the potential for physical activity or the survival time are to be answered but can also be relevant in a clinical context. Clinicians should be aware of the possibility of cortical contusion zones and deep intracerebral haemorrhages remote from the tract even if these changes cannot be demonstrated by imaging techniques. A by-product of the use of imaging techniques is the possibility of effective demonstration of evidence in the courtroom (Harris 1991).

Acknowledgements The support from P.J.T. Knudsen, G. Böckenholt, J. Svender, H.R. Damm, J. Knappworst, A.S. Boese-Karger and R.A. Rasmussen is gratefully acknowledged.

References

Allen IV, Scott R, Tanner JA (1982) Experimental high-velocity missile head injury. Injury 14:183–193

Besenski N, Jadro-Santel D, Jelavic-Koic F, Pavic D, Mikulic D, Glavina K, Maskovic J (1995) CT analysis of missile head injury. Neuroradiology 37:207–211

Carey ME, Sarna GS, Farrel JB, Happel LT (1989) Experimental missile wound of the brain. J Neurosurg 71:754–764

Cooper PR, Maravilla K, Cone J (1979) Computerized tomographic scan and gunshot wounds of the head: indications and radiographic findings. Neurosurgery 4:373–380

Crockard HA, Brown FD, Calica AB, Johns LM, Mullan S (1977) Physiological consequences of experimental cerebral missile injury and use of data analysis to predict survival. J Neurosurg 46:784–794

Dittmann W (1989) Wundballistische Untersuchungen zur Klinik der Schädel-Hirn-Schußverletzungen. Wehrmed Monatsschr 33: 3–14

Fackler ML, Peters CE (1991) The "shock wave" myth. Wound Ballistics Rev 1(1):38–40

Finnie JW (1993) Pathology of experimental traumatic craniocerebral missile injury. J Comp Pathol 108:93–101

Freytag E (1963) Autopsy findings in head injuries from firearms. Statistical evaluation of 254 cases. Arch Pathol (Lond) 76: 215–225

Harris LS (1991) Postmortem magnetic resonance images of the injured brain: effective demonstration in the courtroom. Forensic Sci Int 50:178–185

Harvey EN, Korr IM, Oster G, McMillan JH (1947) Secondary damage in wounding due to pressure changes accompanying the passage of high velocity missiles. Surgery 21:218–239

Henn R, Liebhardt E (1969) Zur Topik außerhalb des Schußkanals gelegener Hirnrindenblutungen. Arch Kriminol 143:188–191

Hollerman JJ, Fackler ML, Coldwell DM, Ben-Menachem Y (1990) Gunshot wounds: 2. Radiology. Am J Radiol 155:691–702

Illchmann-Christ A (1951) Zur Frage der Beurteilung der Handlungsfähigkeit und Lebensdauer nach stumpfen Schädeltraumen. Arch Orthop Unfallchir 44:586–605

Karger B (1995) Penetrating gunshots to the head and lack of immediate incapacitation. I. Wound ballistics and mechanisms of incapacitation. Int J Legal Med 108:53–61

Karger B, Nüsse R, Schroeder G, Wüstenbecker S, Brinkmann B (1996) Backspatter from experimental close-range shots to the head. I. Macrobackspatter. Int J Legal Med 109:66–74

Kaufman HH, Loyola WP, Makela ME, Frankowsky RF, Wagner KA, Bustein DP, Gildenberg PC (1986) Gunshot wounds to the head: a perspective. Neurosurgery 18:689–695

Kirkpatrick JB, DiMaio VJM (1978) Civilian gunshot wounds of the brain. J Neurosurg 48:185–198

Klaue R (1949) Die indirekten Frakturen der vorderen Schädelgrube beim Schädeldachschuß. Dtsch Z Nervenheilkd 161:167–193

Knudsen PJT, Svender J (1994) Doppler radar velocity measurements for wound ballistics experiments. Int J Legal Med 107: 1–6

Levett JM, Johns LM, Replogle RL, Mullan S (1980) Cardiovascular effects of experimental cerebral missile injury in primates. Surg Neurol 13:59–64

Lorenz R (1948) Der Schußkanal im Röntgenbilde. Dtsch Z Gerichtl Med 39:435–448

Messmer JM, Fierro MF (1986) Radiologic forensic investigation of fatal gunshot wounds. Radiographics 6:457–473

Metter D, Stute H, Rauschke J (1988) Rechtsmedizinische Röntgenuntersuchungen bei Schädelschüssen. Beitr Gerichtl Med 47:473–477

Petersohn F (1967) Über die Aktions-und Handlungsfähigkeit bei schweren Schädeltraumen. Dtsch Z Gerichtl Med 59:259–270

Rodieck SO (1984) Computertomographische Klassifikation von Kopfschußverletzungen. Fortschr Röntgenstr 141:11–17

Schmidt G, Kallieris D (1982) Use of radiographs in the forensic autopsy. Forensic Sci Int 19:263–270

Schumacher M, Oehmichen M, König HG, Einighammer H, Bien S (1984) Computertomographische Untersuchungen zur Wundballistik kranialer Schußverletzungen. Beitr Gerichtl Med 43: 95–101

Seidel BU, Vogelsang H, Galanski M (1983) Computertomographische Befunde und Verlaufskontrollen bei Schädel-Hirn-Schußverletzungen. Neurochirurgia 26:172–176

Siccardi D, Cavaliere R, Pau A, Lubinu F, Turtas S, Viale GL (1991) Penetrating craniocerebral missile injuries in civilians. A retrospective analysis of 314 cases. Surg Neurol 35:25–33

Smith AS, Hurst GC, Duerk JL, Diaz PJ (1991) MR of ballistic materials: imaging artifacts and potential hazards. Am J Neuroradiol 12:567–572

Spatz H (1941) Gehirnpathologie im Kriege. Von den Gehirnwunden. Zentralbl Neurochir 6:162–212

Teitelbaum GP, Yee CA, Van-Horn DD, Kim HS, Colletti PM (1990) Metallic ballistic fragments: MR imaging safety and artifacts. Radiology 175:855–859

Watkins FP, Pearce BP, Stainer MC (1988) Physical effects of the penetration of head simulants by steel spheres. J Trauma Suppl 28(1):S40–S54

Wüllenweber R, Schneider V, Grumme T (1977) Computertomographische Untersuchungen bei Schädel-Schuß-Verletzungen. Z Rechtsmed 80:227–246